Understanding real-world variability of hybrid electric vehicle fuel economy

Hillol Kumar Roy[1], Andrew McGordon[2], Paul Jennings[2]

[1]TVS Motor Company Limited, India, [2]The University of Warwick, UK

Abstract

The variability of fuel economy (FE) is of significant importance as that of average FE to realize FE benefits of hybrid electric vehicles (HEVs) consistently by all users in the real-world. Over the years, majority of the research has been focused on improving average FE overlooking the variability. Although in recent years, few studies have been focused on the reduction of FE variability, no study has been concentrated to understand why certain design has lower FE variability as that of others. This paper provides a detail analysis to decipher the reasons for the FE variability in the real-world. This study considered the optimum designs based on two established design optimization methodologies considering Toyota Prius non plug-in hybrid as a base vehicle. This study analyses the impacts of the parameters of driving patterns and the operation of powertrains on FE variability. The study explains that comparatively bigger internal combustion engine (ICE) in combination with the optimum sizes of generator-motor and battery could lead to lower FE variability in the real-world due to lesser time of operation of ICE to charge the battery.

1. Introduction

Significant effects of fossil fuels on global emissions and a predicted scarcity of fossil fuel reserves [1], [2] has inspired researchers to look for solutions to reduce fuel dependence. Hybrid electric vehicle (HEV), generally combining an internal combustion engine (ICE) and electric machines is a proven technology for the improvement of fuel economy (FE) and the reduction of emissions [3]. Long driving range of an ICE and low emissions of an electric machine, makes HEVs beneficial over conventional ICE powered vehicles.

HEVs generally have higher FE compared to conventional vehicles [4] due to the use of ICE and electric machines at their most efficient points in their operating regimes. But FE variability i.e., variation in FE due to different factors exists in HEVs [5-10], as it does in conventional vehicles [11]. Considerable variation exists between customers' reported real-world FE and declared FE by the manufacturers [12]. FE variability exists due to factors such as variation in operation of air-conditioning [5], atmospheric temperature [6-8], and driving patterns [9], [10]. Driving patterns are generally considered as speed-time profiles of a vehicle [13-15], Among all the factors, the variation in driving patterns not only depends on driving styles but also external factors such as traffic conditions [16]. As a result, driving patterns vary from person to person, vehicle to vehicle, and even time to time. Evidence indicates that HEVs have higher FE variability due to variation in driving patterns compared to conventional vehicles [17-19], but no analysis has been found to explore the reasons for the variability. Research studies have been conducted over the years for the improvement of FE in HEVs [20-31], however, FE variability has been overlooked. In few recent papers [32-34] a design optimisation methodology has been proposed to reduce FE variability in real-world. Although the studies [32-34] showed the potential of design optimization methodologies for the reduction of FE variability in the real-world, the papers did not discuss much details of the underlying reasons for the variability. The higher FE variability combining with higher cost of HEVs compared to conventional vehicles could cause higher customer dis-satisfaction in case of HEVs. No other previous research paper has been found putting much focus to analyze the reasons for FE variability in the real-world. This paper analyses statistically to understand the reasons for FE variability considering the optimum designs of the two design optimization methodologies discussed in the previous papers [32-34] . This paper provides a direction to choose the optimum design for customer satisfaction in the real-world.

2. Methodology

2.1 Vehicle Architecture

A non-plug-in Toyota Prius NHW10 HEV is considered as a vehicle to understand the FE variability. A simulation model of the vehicle from Warwick Powertrain Simulation Tool for Architectures (WARPSTAR) [35], based on MATLAB-Simulink, was considered for the study. The simulation model of the Toyota Prius was considered as a benchmark vehicle for comparison. The vehicle simulation model of the Toyota Prius consisted of the following major parameters.

- Vehicle mass: 1368 kg
- Rolling resistance coefficient: 0.009
- Body aerodynamic drag coefficient: 0.29
- Vehicle frontal area: 2.0 m^2
- Transmission: Power-split
- Internal combustion engine (ICE): 43 kW, spark ignition
- Generator: 15 kW, permanent magnet direct current
- Motor: 30 kW, permanent magnet direct current
- Battery: 6 Ah, NiMH
- Initial battery state of charge (SOC): 0.7

2.2 Supervisory Control Strategy

The control strategy of the Toyota Prius used for this study was the in-built control strategy available in the WARPSTAR [35]. It was a rule-based electric assist charge sustaining supervisory control strategy for energy management [30].

The supervisory control strategy consisted of the following rules.

- The electric motor supplied all the driving torque if the battery SOC was higher than SOC_L and the vehicle speed was below a certain minimum speed V_C or the required torque was smaller than T_C.
- When the required torque was higher than T_C and the engine operated in its efficient region with the required driving torque, the engine produced the torque to drive the vehicle alone.
- When the required torque was higher than the maximum torque of the engine at the engine's operating speed, the motor provided the additional torque.
- When the battery SOC was lower than SOC_L, the engine provided additional torque, which was used by the motor to recharge the battery.
- When the battery SOC was lower than SOC_H, the motor charged the battery by regenerative braking.

SOC_L: lowest desired battery SOC;

SOC_H: highest desired battery SOC;

V_C: vehicle speed below which the vehicle operated in electric-only mode;

T_C: required vehicle torque below which the vehicle operated in electric-only mode.

2.3 Problem Formulation & Objective Function

The problem was formulated as a constraint optimization problem where an optimum combination of ICE, generator, motor, and battery is needed to find the optimum FE without sacrificing vehicle performance. The study considered FE as the objective function to be minimized.

The problem was formulated as follows:

Minimize, $f(x),\ x \in X$

Satisfy, $h_i(x) \leq 0,\ i = 1, 2, .., N$

Where,

x is the solution to the problem within the solution space X,

X is the upper and lower limit of the design variables,

$f(x)$ is the objective function,

$h_i(x)$ represents the constraints,

N is the number of constraints.

2.4 Design parameters

The study considered five parameters, four powertrain components (ICE, generator, motor, and battery) and a parameter (Target SOC) of supervisory control strategy, to find an optimum design. The maximum power of the internal combustion engine (ICE) (P_{ICE}), the maximum power of the generator (P_G), the maximum power of the motor (P_M), and the maximum capacity of the battery (C_B) were considered as design parameters to be optimized. As the main purpose of this research study was to understand the reasons for FE variability in the real-world, the consideration of only power of component was sufficient for initial study. Other parameters of the components could be considered in future study.

The components of the Toyota Prius HEV were considered as the base components for this study. The fuel consumption and efficiency maps of Toyota Prius are shown in Figure 1 and Figure 2. Different power ratings of the components during optimization were achieved by linear scaling of the performance of the base components [21], [23], [26].

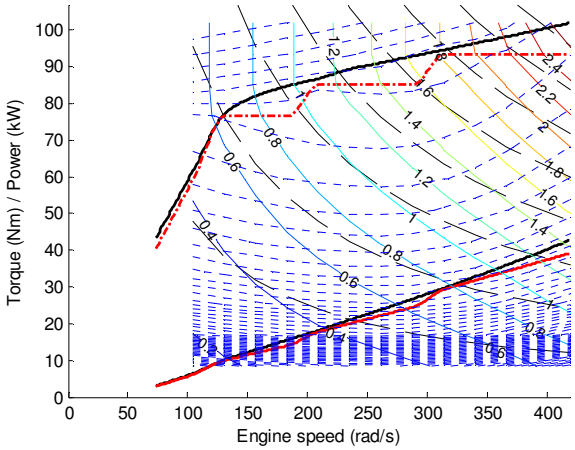

Figure 1: Engine fuel consumption map (in g/s) of Toyota Prius

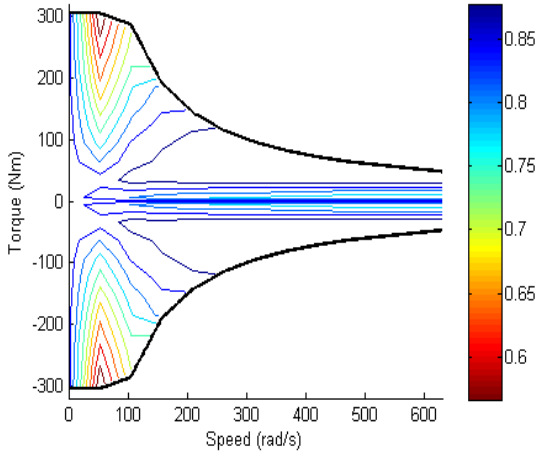

Figure 2: Motor efficiency map of Toyota Prius

The ranges of the variations of each design parameters for powertrain components were kept within ±70% of the base component, as shown in Table 1.

Table 1. Ranges of design parameters

Design parameter	Lower limit	Upper limit
P_{ICE}, kW	12.9	73.1
P_M, kW	9.0	51.0
P_G, kW	4.5	25.5
C_B, Ah	1.8	10.2
Target SOC	0.0	1.0

The lower and upper limits for the parameter (Target SOC) of the supervisory control strategy were considered with the widest possible range (from 0 to 1) to enable the optimization algorithm to find the global optimum.

2.5 Constraints

Acceleration, maximum speed, and gradeability were considered as constraints so that the performance of the optimum design should not be inferior compared to the benchmark vehicle, Toyota Prius HEV. These performance constraints were calculated based on the suggestions found in [36, 37]. The constraints for this study were as follows.

- Acceleration (0 ~ 60 mph): < 13.4 seconds
- Maximum speed: > 113.3 mph
- Gradeability: > 13.8% @ 55 mph
- Delta SOC (Difference between final and initial battery SOC): < 0.5%

The delta SOC was considered in order to eliminate the effect of battery SOC on FE while comparing different designs for FE performance. The initial and final battery SOC over all driving patterns need to be same to eliminate the influence of battery SOC on FE [27].

2.6 Optimization Method

A genetic algorithm (GA) was considered as optimization method [32, 38-40]. Each optimization variable consisted of 8 bits. Single point crossover was used and the crossover probability was considered as 0.9. The mutation probability was considered as 0.15. The roulette wheel method was used as the selection method. The population size was considered 50. The number of generations was considered 250 as there was little improvement of results after 200 generations. The total number of generations was considered as optimization termination criterion i.e., optimization terminated after 250 generations.

Since, the GA is stochastic in nature, each optimization run does not show same result and there is no simple method to verify for a component size optimization problem whether the solution reaches the global optimum. Therefore, each optimization run was carried out 10 times and the optimum design with the minimum FE value was presented as a result.

2.7 Optimization Approach

This study also used model-in-loop approach [41] where an optimization method works along with a vehicle simulation model and this is a preferred time and cost saving method.

2.8 Optimum Design

The optimization of powertrain components was conducted using two methodologies which are termed as M1 and M2, respectively [32]. The M1 methodology considers a single driving pattern for the optimization of powertrain component sizes, whereas, the M2 methodology categorizes driving patterns into different traffic conditions and driving styles and considers all the categorized driving patterns simultaneously for the optimization of powertrain component sizes. The study considered one normal urban driving pattern – FTP-75, one aggressive urban driving pattern – LA92, one normal highway driving pattern – HWFET, one aggressive highway driving pattern – US06 and one conservative driving pattern – NEDC which consisted of urban (ECE15) as well as highway (EUDC) driving. The M1 methodology considered each of the five driving patterns separately for the optimization and the M2 methodology considered all the five driving patterns simultaneously for the optimization. For the M1 methodology, FE was minimized over a single driving pattern, whereas, for the M2 methodology, overall FE over the five driving patterns was minimized. All the five driving patterns had equal weight for the M2 methodology.

The optimum designs of both the M1 and M2 methodologies are shown in Table 2. The optimum designs based on the M1 methodology over the NEDC, FTP, LA92, HWFET, and US06 are termed as M1-NEDC, M1-FTP, M1-LA92, M1-HWFET, and M1-US06, respectively. The optimum design of the M2 methodology is termed as M2.

Table 2: Comparison of optimum component sizes: Toyota Prius, M1 methodology, and M2 methodology [32], [33]

Design parameter	Toyota Prius (Bench-mark vehicle)	Optimum component sizes					
		M1 methodology					M2 methodology
		M1-NEDC	M1-FTP	M1-LA92	M1-HWFET	M1-US06	M2 design
P_{ICE}, kW	43.0	35.1	37.9	36.3	29.3	40.5	44.9
P_G, kW	15.0	13.2	14.1	13.7	12.2	18.3	16.5
P_M, kW	30.0	39.9	39.5	44.4	44.3	34.8	30.5
C_B, Ah	6.0	6.2	8.9	8.7	7.3	8.7	7.7

2.9 Real-world Driving Patterns

Speed-time data logged for a conventional vehicle (i.e., ICE powered only) driven by 10 drivers was considered as real-world driving data. The vehicle was driven over a predefined route consisting of urban and highway driving in the area of Coventry, United Kingdom. The route started and finished at the University of Warwick, United Kingdom. It passed through Kenilworth, Leamington Spa, and Coventry. The 10 driving patterns were termed as DP1 to DP10, respectively. Driving parameters of the 10 driving patterns are shown in Table 3.

The study assumed that speed-time profiles of a vehicle were independent of the type of vehicle. Although the data was collected for a conventional vehicle, with the assumption of independency of speed-time data from type of vehicle, the vehicle's speed-time data could be considered as driving patterns in real-world driving conditions for an initial study to validate the new methodology (M2) in the real-world.

Table 3: Driving parameters of real-world driving patterns [33]

Driving parameters	**Driving patterns**									
	D1	**D2**	**D3**	**D4**	**D5**	**D6**	**D7**	**D8**	**D9**	**D10**
Total distance, miles	27.4	27.4	27.5	27.2	27.4	27.4	27.4	27.4	27.4	27.4
Total time, seconds	3560	4059	3862	3763	3644	4065	3826	3799	3898	4053
Driving time, seconds	3062	3571	3417	3407	3303	3526	3373	3423	3349	3590
Drive time spent accelerating, seconds	1369	1490	1546	1601	1400	1494	1589	1540	1500	1601
Drive time spent decelerating, seconds	1371	1668	1639	1498	1523	1823	1482	1506	1558	1714
% of driving time accelerating	44.7	41.7	45.2	47.0	42.4	42.4	47.1	45.0	44.8	44.6
% of driving time decelerating	44.8	46.7	48.0	44.0	46.1	51.7	43.9	44.0	46.5	47.7
Maximum acceleration, m/s^2	3.31	2.26	3.34	2.45	3.40	3.17	2.68	2.51	2.39	2.38
Maximum speed, mph	79.1	77.6	86.9	75.3	83.0	85.6	74.8	74.1	74.2	73.9
Average speed, mph	27.7	24.3	25.6	26.0	27.1	24.3	25.7	26.0	25.3	24.3

Where,

$$Driving\ time\ accelerating = \frac{Drive\ time\ spent\ accelerating}{Driving\ time}$$

$$Driving\ time\ decelerating = \frac{Drive\ time\ spent\ decelerating}{Driving\ time}$$

2.10 Fuel Economy Evaluation

Each optimum design of both the M1 and M2 methodologies was evaluated for FE over the 10 real-world driving patterns. Coefficient of variation of FE over the 10 driving patterns was considered as FE variability of an optimum design. The coefficient of variation is the ratio of standard deviation to mean.

To compare different optimum designs for FE, the initial and final battery SOC should be same, as the battery SOC is closely related to ICE operation, which is responsible for FE. In this study, the final battery state of charge (SOC) of each optimum design after the end of each driving pattern was maintained within < 0.5% of the initial battery SOC i.e., delta SOC < 0.5%. The final battery SOC was maintained by controlling the target SOC of the supervisory control strategy by trial and error method [32]. Although, the final battery SOC could be also achieved by an optimization method and could be used for practical application. However, in this study, the main focus was to evaluate methodologies; hence, the type of evaluation method used was of little significance.

The FE values of the M2 design compared to the Toyota Prius and optimum designs of the M1 methodology over the 10 real-world driving patterns are shown in Table 4 [33]. The M2 design had 5.3% lower FE variability and 0.2% higher average FE compared to the Toyota Prius. The M2 design reduced FE variability by 48.9, 33.3, 46.7, 22.2, and 18.9% compared to the M1-NEDC, M1-FTP, M1-LA92, M1-HWFET, and M1-US06 designs, respectively. The M1-NEDC, M1-FTP, M1-LA92, M1-HWFET, and M1-US06 had 41.1, 26.3, 38.9, 15.8, and 12.6%, respectively higher FE variability compared to the Toyota Prius.

Table 4: FE over real-world driving patterns: Toyota Prius, M1 methodology, and M2 methodology[33]

Driving pattern	Fuel economy (FE), miles per gallon (mpg)						
	Toyota Prius	M1 methodology					M2 methodology
		M1-NEDC	M1-FTP	M1-LA92	M1-HWFET	M1-US06	M2 design
D1	54.9	48.6	50.7	49.1	47.1 (*)	52.3	55.4
D2	64.9	64.3	66.7	65.6	57.7	66.1	65.0
D3	50.7	48.7	51.7	50.4	47.5 (*)	52.0	51.1
D4	64.5	66.0	67.2	66.9	60.1	66.1	64.1
D5	57.4	54.5	56.6	55.9	50.1 (*)	57.0	57.4
D6	50.4	46.3	49.2	47.4	47.3 (*)	49.9	51.0
D7	59.3	58.9	60.6	60.4	53.5	59.9	58.8
D8	68.1	70.9	71.4	71.5	66.0	69.6	67.5
D9	60.2	59.9	62.6	62.2	52.9 (*)	61.9	60.9
D10	60.0	61.4	62.5	62.3	55.9	61.1	59.6
Maximum FE, mpg	68.1	70.9	71.4	71.5	66.0	69.6	67.5
Minimum FE, mpg	50.4	46.3	49.2	47.4	47.1	49.9	51.0
Average FE, mpg	59.0	58.0	59.9	59.2	53.8	59.6	59.1
Standard deviation of FE, mpg	5.6	7.8	7.2	7.8	5.9	6.4	5.3
FE variability, %	9.5	13.4	12.0	13.2	11.0	10.7	9.0
(*): Failed to operate charge sustaining							

$$FE\ variability, \% = \frac{Standard\ deviation\ of\ FE}{Average\ FE} * 100$$

3. Results & Discussion

3.1 Understanding the effect of driving parameters on FE variability

The probable reason for the minimum FE over D6 was due to the higher aggressiveness of D6 compared to other driving patterns. D6 had the second highest maximum speed and second highest maximum acceleration, as shown Figure 3 and Figure 4. D6 had the highest percentage of driving time for acceleration and deceleration among all the driving patterns, as shown in Figure 5. D3 also had higher aggressiveness in driving. D3 had the highest maximum speed (Figure 3), the third highest maximum acceleration (Figure 4), and the second highest percentage of time for acceleration and deceleration (Figure 5). For this reason, the Toyota Prius, M2, and M1-US06 designs provided the second lowest FE and M1-NEDC, M1-FTP, and M1-LA92 designs provided the third lowest FE over D3.

D8 had the second lowest maximum speed (Figure 3) and second lowest maximum acceleration (Figure 4). D8 also had the third lowest percentage of time for acceleration and deceleration (Figure 5). Therefore, D8 was lesser aggressive compared to other driving patterns and this was probably the reason for the highest FE of all optimum designs over D8.

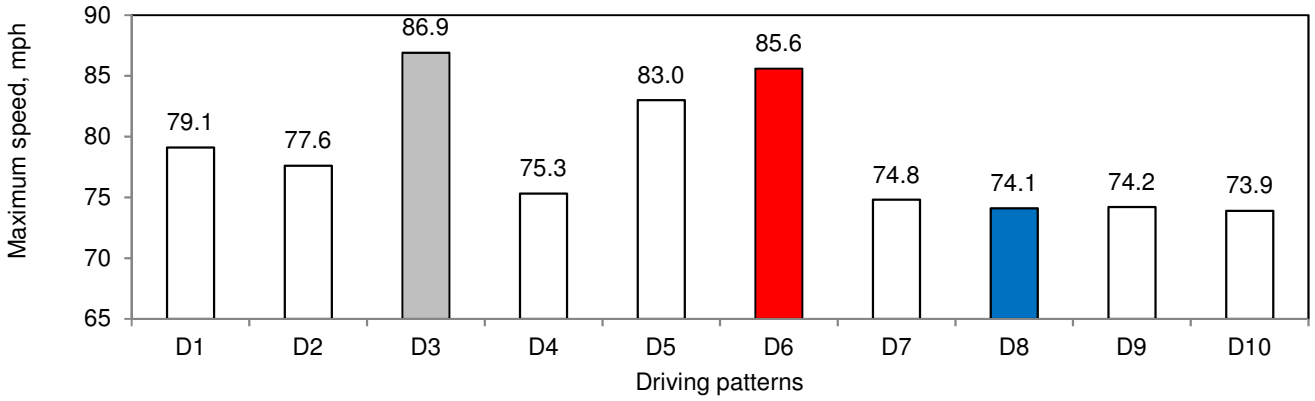

Figure 3: Maximum speed; D1 to D10 driving patterns

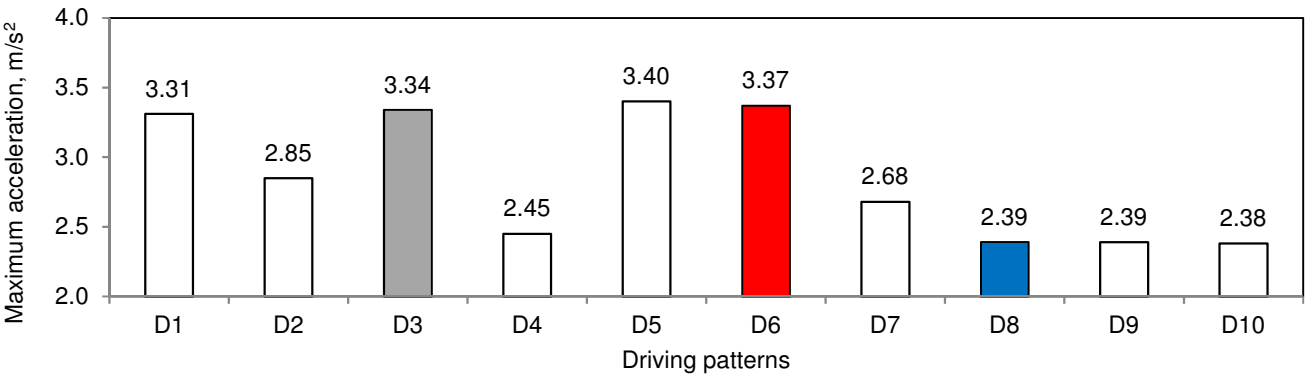

Figure 4: Maximum acceleration: D1 to D10 driving patterns

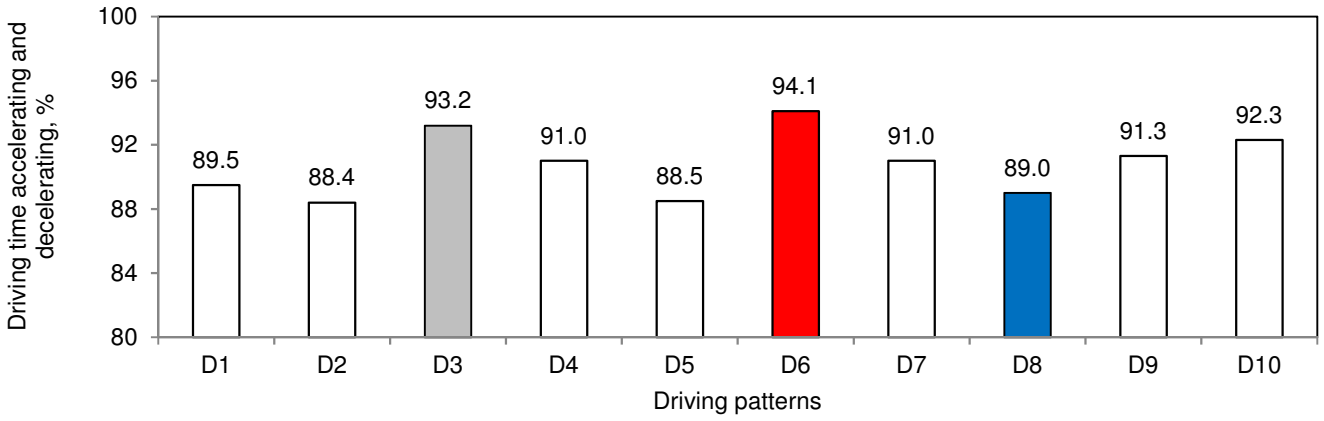

Figure 5: Time for acceleration and deceleration: D1 to D10 driving patterns

3.1.1 Comparison of FE: M2 and Toyota Prius

The M2 design had 0.9, 0.2, 0.8, 1.2, and 1.2% higher FE over D1, D2, D3, D6, and D9, respectively compared to the Toyota Prius. But the M2 design had 0.6, 0.8, 0.9, and 0.7% lower FE over D4, D7, D8, and D10 respectively compared to the Toyota Prius. The M2 design and Toyota Prius provided same FE over D5. The M2 design had higher FE over 5 driving patterns and lower FE over 4 driving patterns compared to the Toyota Prius.

D1, D2, D3, and D6 driving patterns had higher maximum speed and maximum acceleration compared to D4, D7, D8, and D10. D1, D2, D3, D6, and D9 also had more percentage of driving time for deceleration compared to D4, D7, and D8. But D4, D7, D8, and D10 had more percentage of driving time for acceleration compared to D2 and D6. The higher deceleration time in D1, D2, D3, D6, and D9 indicated potentially higher traffic on the road. The higher driving time for acceleration with lesser time for deceleration in D4, D7, and D8 indicated lesser traffic. Therefore, the M2 design had better FE compared to the Toyota Prius, if driving patterns consisted of higher maximum speed, maximum acceleration, and traffic. Hence, the M2 design had higher potential for better FE over aggressive driving patterns and more suitable for real-world applications compared to the Toyota Prius.

3.1.2 Comparison of FE: M2 and M1

The M2 design had higher FE over D1, D5, and D6 compared to all the designs of M1 methodology. D1, D5, and D6 had higher maximum speed and maximum acceleration compared to D2, D4, D7, D8, D9, and D10 driving patterns. Therefore, the M2 design had higher chances of better FE compared to the designs of M1 methodology, if driving patterns consisted of higher maximum speed and acceleration. Although D3 also had higher maximum speed and maximum acceleration compared to D2, D4, D7, D8, D9, and D10 driving patterns, the M1-FTP and M1-US06 designs had higher FE compared to the M2 design. No conclusion can be drawn in terms of the percentage of time spent for acceleration and deceleration.

3.2 Understanding the effect of powertrain operation on FE variability

As the M2 design had the highest FE over D1 and D6 compared to other designs, the D1 driving pattern was chosen to understand the higher FE of the M2 design compared to other designs. The M2 design had 14.0, 9.3, 12.8, and 5.9% higher FE over D1 driving pattern compared to the M1-NEDC, M1-FTP, M1-LA92, and M1-US06 designs, respectively. The M1-NEDC and M1-US06 designs were chosen for the comparison with the M2 design due to the highest and lowest difference in FE compared to the M2 design. The M2 design also had 0.9% higher FE compared to the Toyota Prius. The M2 design was also compared with the Toyota Prius to analyze the difference in FE.

3.2.1 Comparison over D1: M2 and M1-NEDC

The FC values of the M2 and M1-NEDC designs over D1 are compared in Figure 6. The FC of the M2 design at high speed regions (between 2430 and 2730 seconds) spread up to 2.87 g/s but majority of the FC concentrated between 0.5 to 1.7 g/s, whereas the FC of the M1-NEDC design at the same speed range spread up to 2.24 g/s and majority of the FC happened at 2.24 g/s. Apart from the high speed regions (between 2430 and 2730 seconds), the FC of the M1-NEDC design concentrated more between 0.5 and 1.5 g/s. In the lower speed region, the FC of the M2 design spread up to 2.87 g/s but a portion of the FC happened up to 0.5 g/s.

As the fuel consumption (FC) directly depends on the operation of ICE, the torque and speed of the ICE for the M2 and M1-NEDC designs over D1 driving pattern are shown in Figure 7 and Figure 8, respectively. Figure 7 shows that the M1-NEDC design operated more time between 60 Nm to 83.2 Nm (the maximum torque corresponding to the maximum power 35.12 kW), whereas, the operation of the M2 design spread all over the range between 0 Nm to 106.6 Nm (the maximum torque corresponding to the maximum power 44.94 kW). The M1-NEDC design operated comparatively higher times at higher speed compared to the M2 design, as shown in Figure 8.

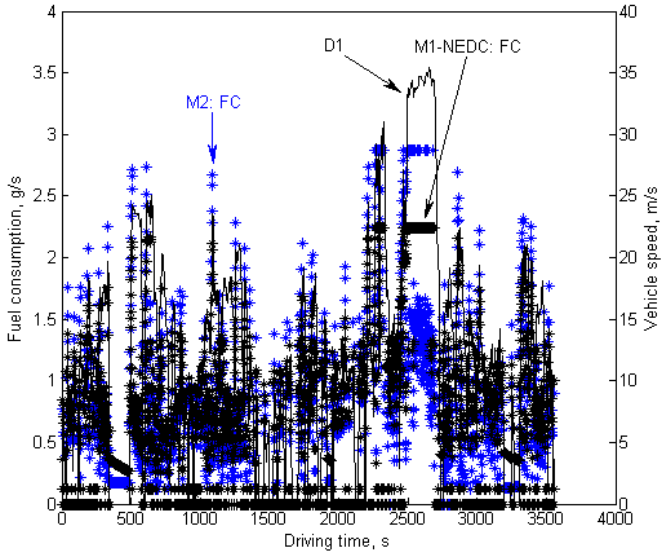

Figure 6: Comparison of fuel consumption over D1: M2 and M1-NEDC designs

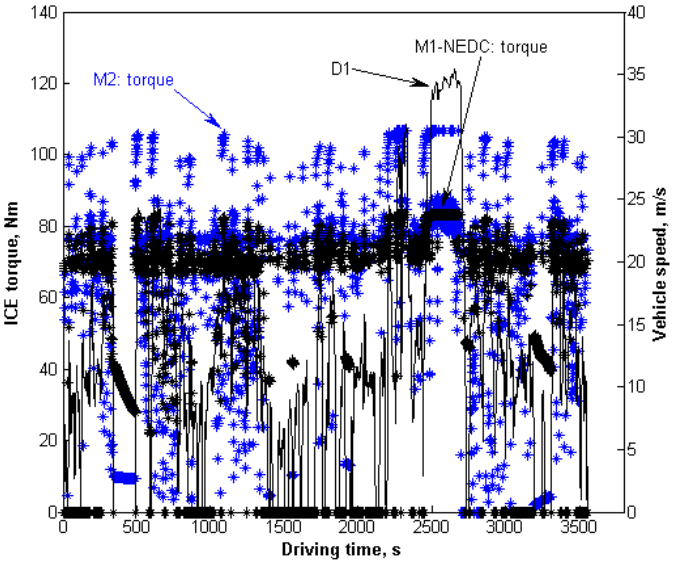

Figure 7: Comparison of ICE torque over D1: M2 and M1-NEDC designs

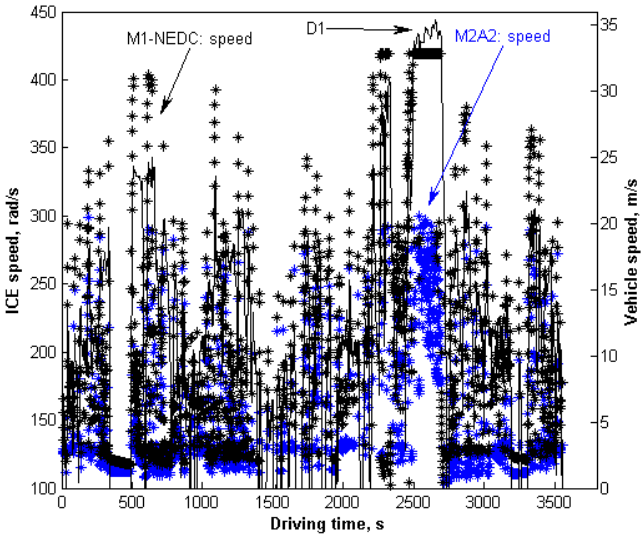

Figure 8: Comparison of ICE speed over D1: M2 and M1-NEDC designs

Although Figure 6 shows the comparison of FC between the M2 and M1-NEDC designs, it cannot be concluded directly which design is better in terms of FC? Therefore, the FC of both the designs with respect to torque and speed of ICE are compared in Figure 9 and Figure 10, respectively. Even though Figure 7 and Figure 8 show the operation of ICE of the M2 and M1-NEDC designs, it is difficult to analyze how many times ICE has been operated at particular speed and torque, which is important to understand the reason behind difference in FE. Therefore, histogram of the torque and speed of the ICE of the M2 and M1-NEDC designs over D1 driving pattern are plotted in Figure 11 and Figure 12, respectively.

The FC over 60 Nm contributed to 86.3 and 90.6% of total FC for the M2 and M1-NEDC designs respectively, as shown in Figure 9. The M2 design had 49.7% less FC between 60 to 80 Nm compared to the M1-NEDC design, as shown in Figure 9, due to 41.6% less time of operation between 60 to 80 Nm compared to the M1-NEDC design, as shown in Figure 11. Although the M2 design operated 8.5% more time between 80 to 100 Nm compared to the M1-NEDC (Figure 11) but the M2 design had 29.0% less FC between 80 to 100 Nm, as shown in Figure 9, probably due to the operation at higher torque compared to the M1-NEDC design. The M2 design had 16.3% lower FC over 60 Nm compared to the M1-NEDC design due to 19.4% lesser time of operation compared to the M1-NEDC design in this range.

The M2 design had 39.5 and 53.3% less FC between 150 to 200 rad/s and 400 to 450 rad/s respectively (Figure 10) compared to the M1-NEDC design due to 46.8 and 63.7% less time of operation between 150 to 200 rad/s and 400 to 450 rad/s respectively (Figure 12). But the M2 design had 39.7% more FC between 100 to 150 rad/s compared to the M1-NEDC design due to 40.9% more time of operation in this range. The FC above 200 rad/s contributed to 57.6 and 65.5% of total FC for the M2 and M1-NEDC designs, respectively. The M2 design had 22.7% lower FC over 200 rad/s due to 31.3% lower time of operation compared to the M1-NEDC design in this range.

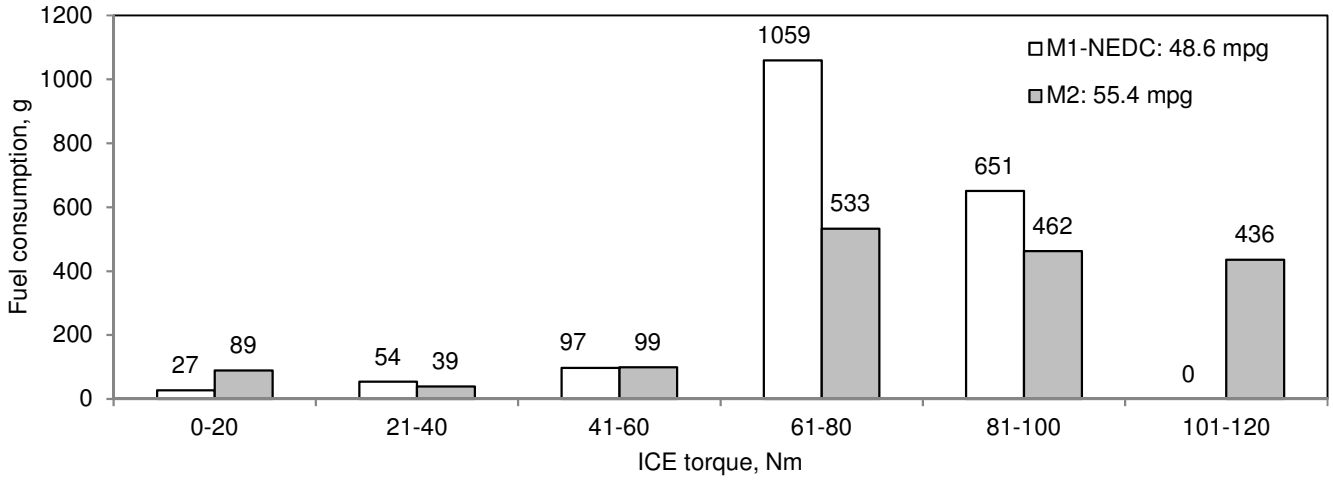

Figure 9: Distribution of fuel consumption w.r.t. ICE torque over D1: M2 and M1-NEDC designs

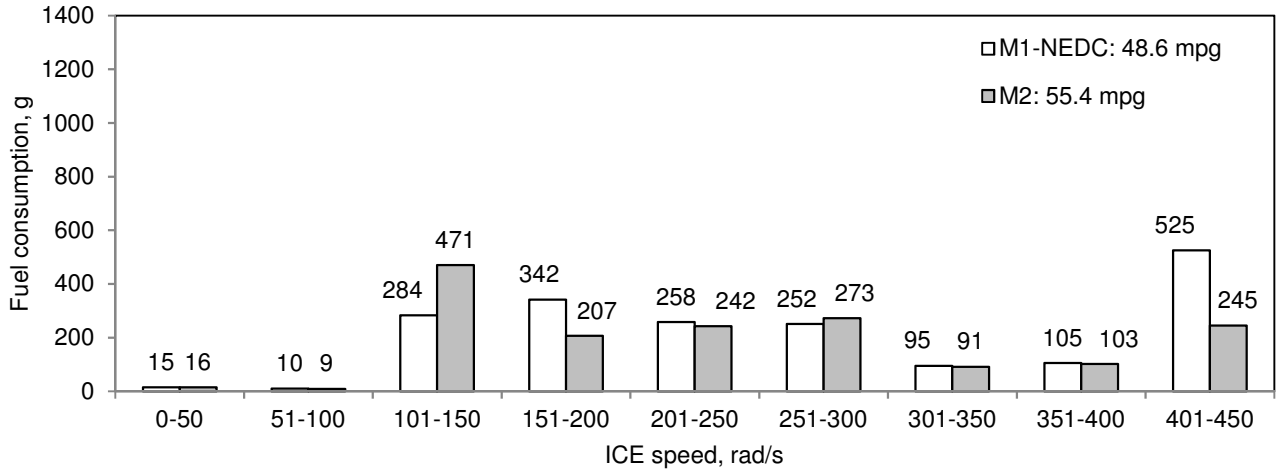

Figure 10: Distribution of fuel consumption w.r.t. ICE speed over D1: M2 and M1-NEDC designs

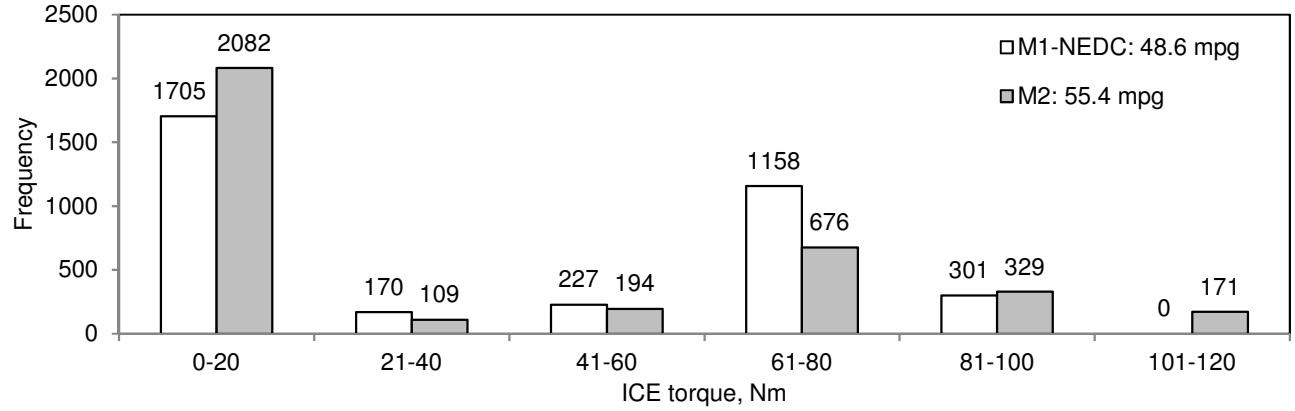

Figure 11: Distribution of ICE torque over D1: M2 and M1-NEDC designs

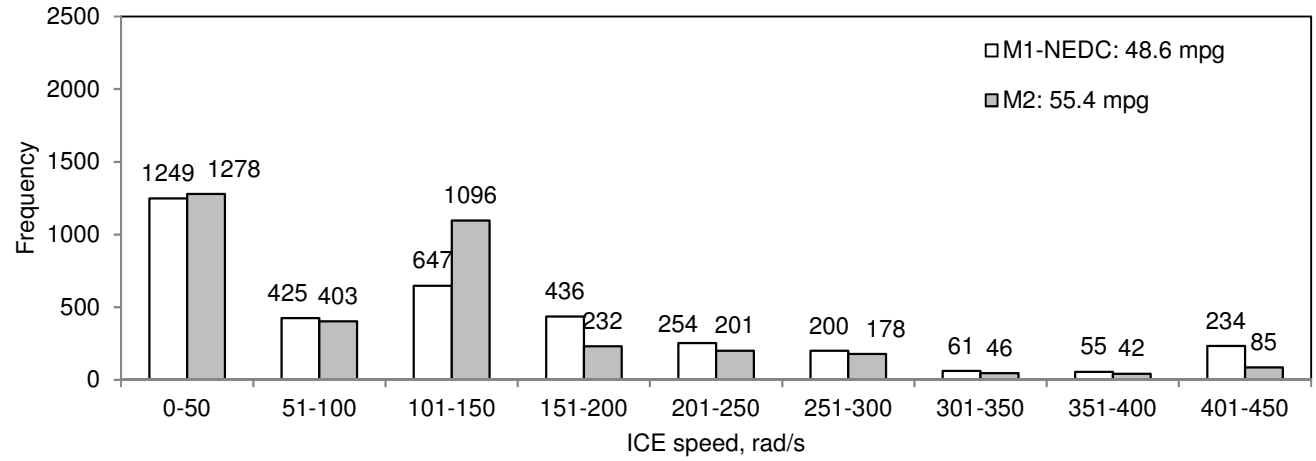

Figure 12: Distribution of ICE speed over D1: M2 and M1-NEDC designs

Due to 27.9% lower ICE power and 24.2% lower battery capacity of the M1-NEDC design compared to the M2 design, the M1-NEDC design was required to operate more time at higher ICE torque (>60 Nm) and speed (>200 rad/s) to achieve the desired final battery SOC. Therefore, more time of usage of the ICE in the M1-NEDC design compared to the M2 design resulted in lower FE in the M1-NEDC design compared to the M2 design.

As the FC over 60 Nm contributed to 86.3 and 90.6% of total FC for the M2 and M1-NEDC designs respectively, 16.3% lower FC over 60 Nm due to 19.4% lesser time of operation over 60 Nm along with 31.3% lower time of operation of ICE over 200 rad/s caused 14.0% higher FE in the M2 design compared to the M1-NEDC design over D1 driving pattern.

3.2.2 Comparison over D1: M2 and M1-US06

The FC values of the M2 and M1-US06 designs over D1 are compared in Figure 13. The FC of the M2 design at high speed regions (between 2430 and 2730 seconds) spread up to 2.87 g/s but majority of FC concentrated between 0.5 to 1.7 g/s, whereas, the FC of the M1-US06 design at the same speed range spread up to 2.59 g/s but has less concentration of FC between 0.5 to 1.7 g/s compared to the M2 design. In the lower speed regions (apart from the high-speed regions between 2430 and 2730 seconds), the spread of FC of the M2 and M1-US06 designs were comparable.

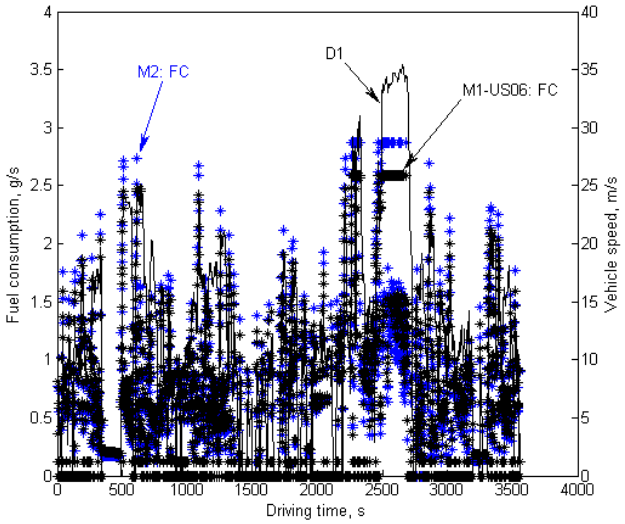

Figure 13: Comparison of fuel consumption over D1: M2 and M1-US06 designs

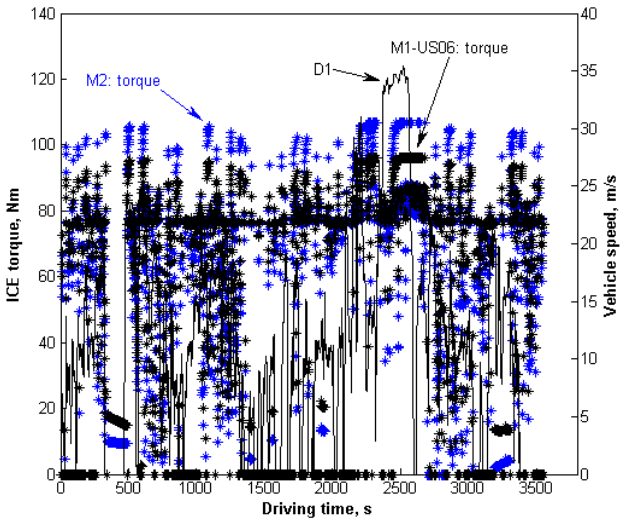

Figure 14: Comparison of ICE torque over D1: M2 and M1-US06 designs

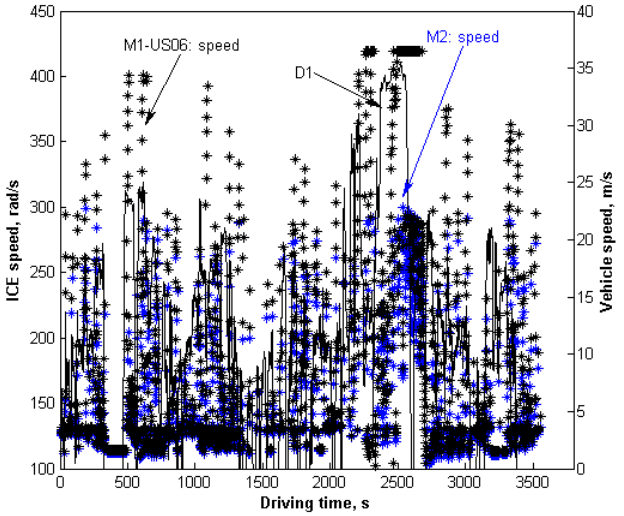

Figure 15: Comparison of ICE speed over D1: M2 and M1-US06 designs

The speed and torque of the ICE for the M2 and M1-US06 designs over D1 driving pattern are shown in Figure 14 and Figure 15, respectively. Figure 14 shows that the operation of the M1-US06 design spread between 0 Nm to 96.0 Nm (the maximum torque corresponding to the maximum power 40.52 kW) and the operation of the M2 design spread between 0 Nm to 106.6 Nm (the maximum torque corresponding to the maximum power 44.94 kW). The M1-US06 design operated comparatively higher times at higher speed compared to the M2 design, as shown in Figure 15.

To understand the distribution of FC between M2 and M1-US06 designs, the FC of both the designs with respect to torque and speed of ICE are compared in Figure 16 and Figure 17, respectively. Similarly, to analyze the operation of ICE, the histogram of the torque and speed of the ICE of the M2 and M1-US06 designs over D1 driving pattern are plotted in Figure 18 and Figure 19, respectively.

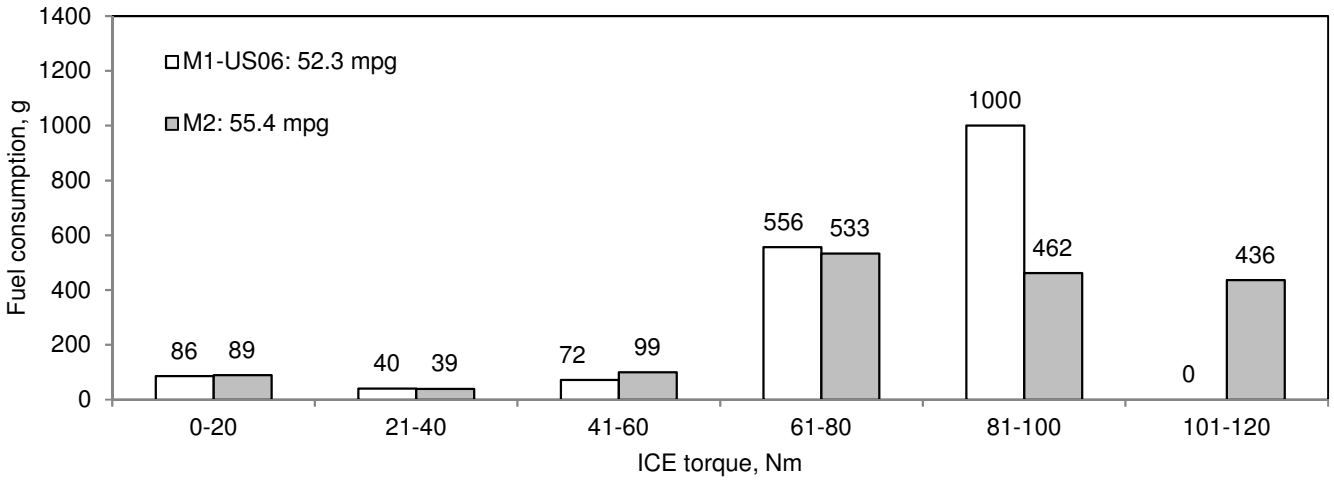

Figure 16: Distribution of fuel consumption w.r.t. ICE torque over D1: M2 and M1-US06 designs

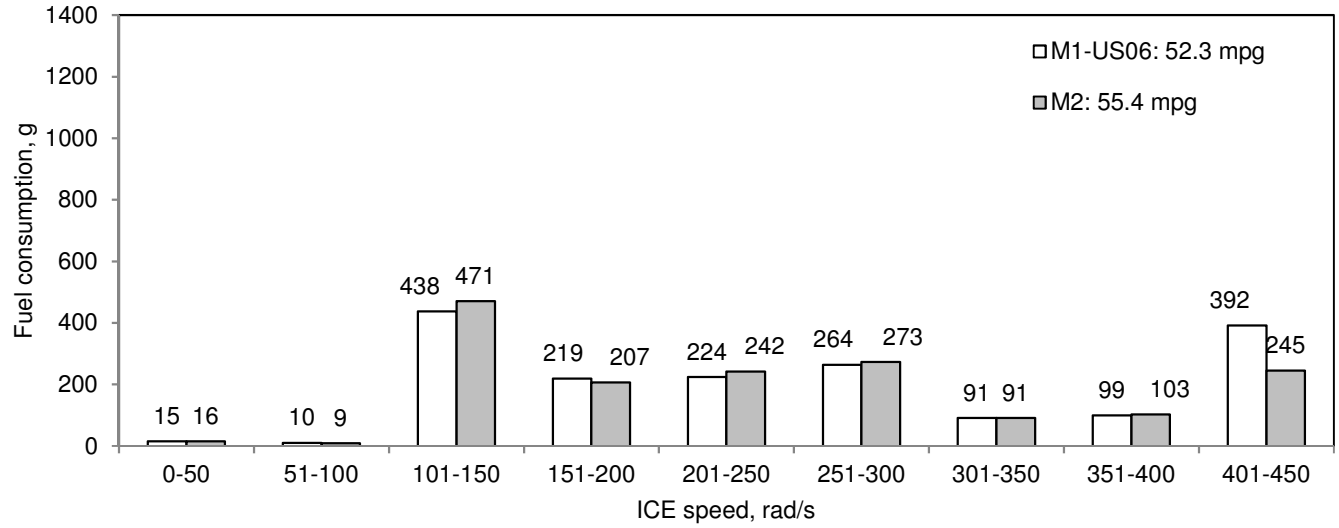

Figure 17: Distribution of fuel consumption w.r.t. ICE speed over D1: M2 and M1-US06 designs

The FC over 60 Nm contributed to 86.3 and 88.8% of total FC for the M2 and M1-US06 designs respectively, as shown in Figure 16. The M2 design had 4.1% less FC between 60 to 80 Nm compared to the M1-US06 design (Figure 16) due to 5.6% less time of operation between 60 to 80 Nm (Figure 18). The M2 design had 53.8% less FC between 80 to 100 Nm (Figure 16) due to 41.3% less time of operation between 80 to 100 Nm compared to the M1-US06 design (Figure 18) The M2 design had 8.1% lower FC over 60 Nm compared to the M1-US06 design (Figure 16) due to 7.8% lower time of operation compared to the M1-US06 design in this range (Figure 18).

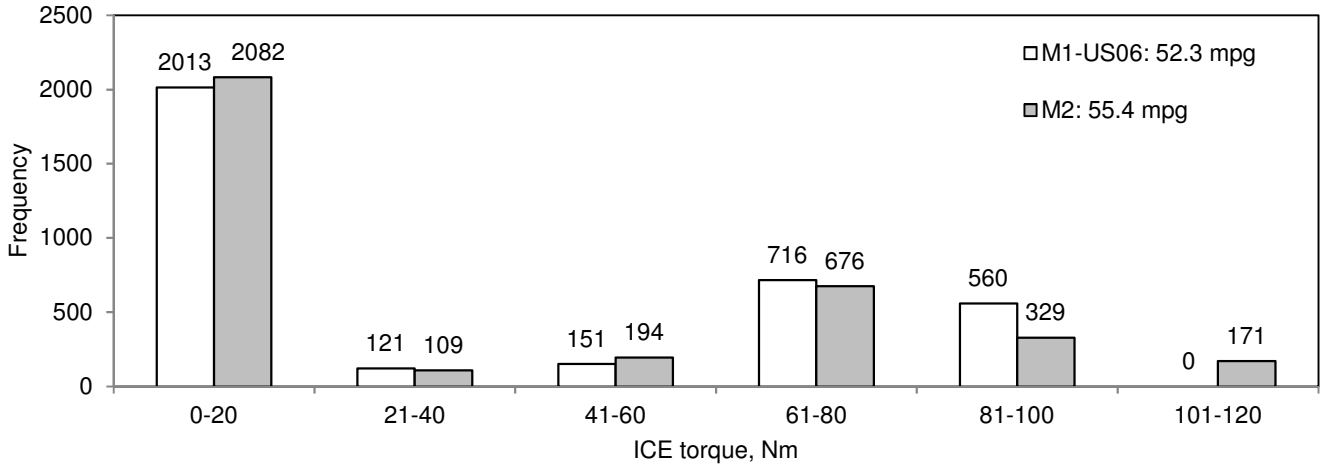

Figure 18: Distribution of ICE torque over D1: M2 and M1-US06 designs

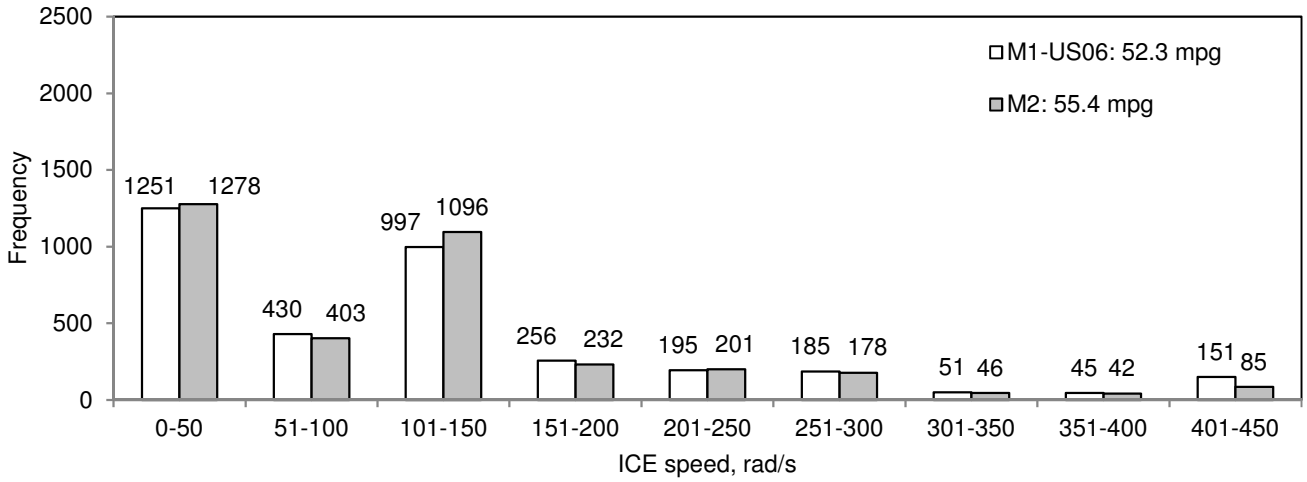

Figure 19: Distribution of ICE speed over D1: M2 and M1-US06 designs

The M2 design had 5.5 and 37.5% less FC between 150 to 200 rad/s and 400 to 450 rad/s respectively (Figure 17) compared to the M1-US06 design due to 9.4 and 43.7% less time of operation between 150 to 200 rad/s and 400 to 450 rad/s respectively (Figure 19). But the M2 design had 7.0% more FC between 100 to 150 rad/s compared to the M1-US06 design due to 9.0% more time of operation in this range. The FC above 200 rad/s contributed 57.6 and 61.1% of total FC for the M2 and M1-US06 designs, respectively. The M2 design had 10.9 % lower FC above 200 rad/s compared to the M1-US06 design due to 12.0% lower time of operation in this range compared to the M1-US06 design.

Although the M1-US06 design had 11.5% higher battery capacity compared to the M2 design, the M1-US06 design was required to operate more time at higher ICE torque and speed to achieve desired final battery SOC due to 10.9% lower ICE power of the M1-US06 design compared to the M2 design. Therefore, more time of usage of the ICE in the M1-US06 design compared to the M2 design resulted in lower FE in the M1-US06 design compared to the M2 design.

As the FC over 60 Nm contributed to 86.3 and 88.8% of total FC for the M2 and M1-US06 designs respectively, 8.1% lower FC over 60 Nm due to 7.8% lesser time of operation over 60 Nm along with 12.0% lower time of operation of ICE over 200 rad/s caused 5.9% higher FE in the M2 design compared to the M1-US06 design over D1 driving pattern.

3.2.3 Comparison over D1: M2 and Toyota Prius

To understand the distribution of fuel consumption between the M2 design and the Toyota Prius, the FC of both the designs with respect to torque and speed of ICE are compared in Figure 20 and Figure 21, respectively. Similar to the previous sections, to understand the engine operation between the M2 design and the Toyota Prius, histogram of the torque and speed of the ICE of the M2 design and Toyota Prius over D1 driving pattern are plotted in Figure 22 and Figure 23, respectively.

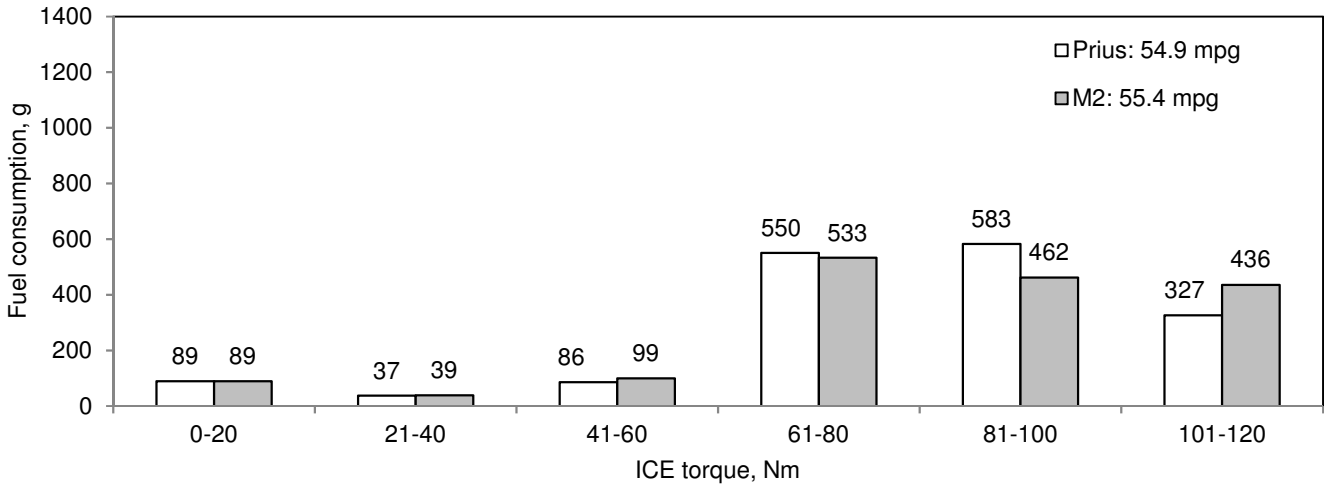

Figure 20: Distribution of fuel consumption w.r.t. ICE torque over D1: M2 design and Toyota Prius

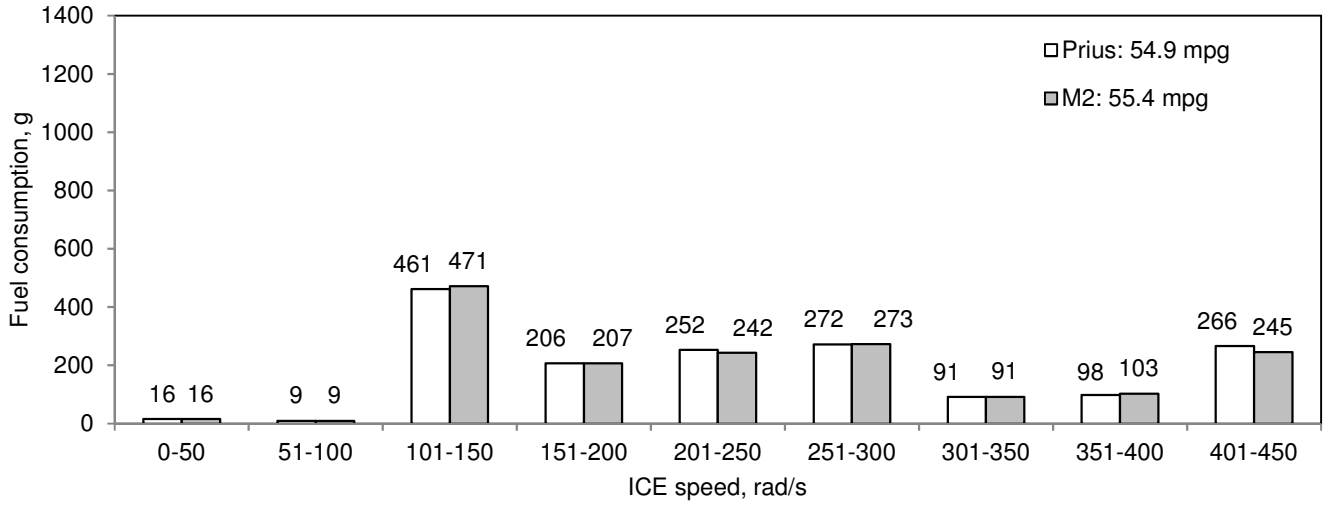

Figure 21: Distribution of fuel consumption w.r.t. ICE speed over D1: M2 design and Toyota Prius

The FC over 60 Nm contributed to 86.3 and 87.3% of total FC for the M2 design and Toyota Prius respectively, as shown in Figure 20. The M2 design had 3.1% less FC between 60 to 80 Nm compared to the Toyota Prius (Figure 20), due to 3.2% less time of operation between 60 to 80 Nm (Figure 22). The M2 design had 20.8% less FC between 80 to 100 Nm (Figure 20) due to 16.7% less time of operation between 80 to 100 Nm compared to the Toyota Prius (Figure 22). But the M2 design had 25.9% more FC between 100 to 120 Nm compared to the Toyota Prius due to 29.2% more time of operation compared to the Toyota Prius in this range. The M2 design had 2.0% lower FC over 60 Nm compared to the Toyota Prius due to 3.1% lower time of operation in this range compared to the Toyota Prius.

The M2 design had 4.0 and 7.9% less FC between 200 to 250 rad/s and 400 to 450 rad/s respectively (Figure 21) compared to the Toyota Prius due to 5.6 and 11.5% less time of operation between 200 to 250 rad/s and 400 to 450 rad/s respectively (Figure 23). But the M2 design had 2.1% more FC between 100 to 150 rad/s compared to the Toyota Prius due to 2.8% more time of operation in this range. Although the M2 and Toyota Prius operated similar period of time between 350 to 400 rad/s, the M2 design had 4.9% higher FC compared to the Toyota Prius, probably due to higher torque operation in this range. All other speed range both the designs had similar FC due to comparatively similar time of operation of ICE. The FC above 200 rad/s contributed 57.6 and 58.6% of total FC for the M2 design and Toyota Prius, respectively. The M2 design had 2.5% less FC compared to the Toyota Prius over 200 rad/s due to 5.0% lower time of operation compared to the Toyota Prius over 200 rad/s.

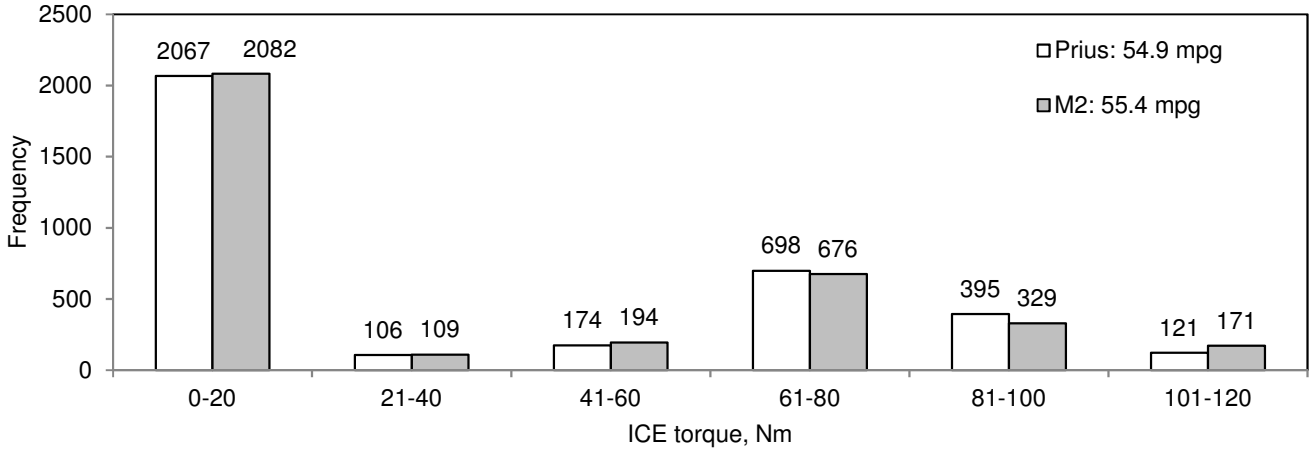

Figure 22: Distribution of ICE torque over D1: M2 design and Toyota Prius

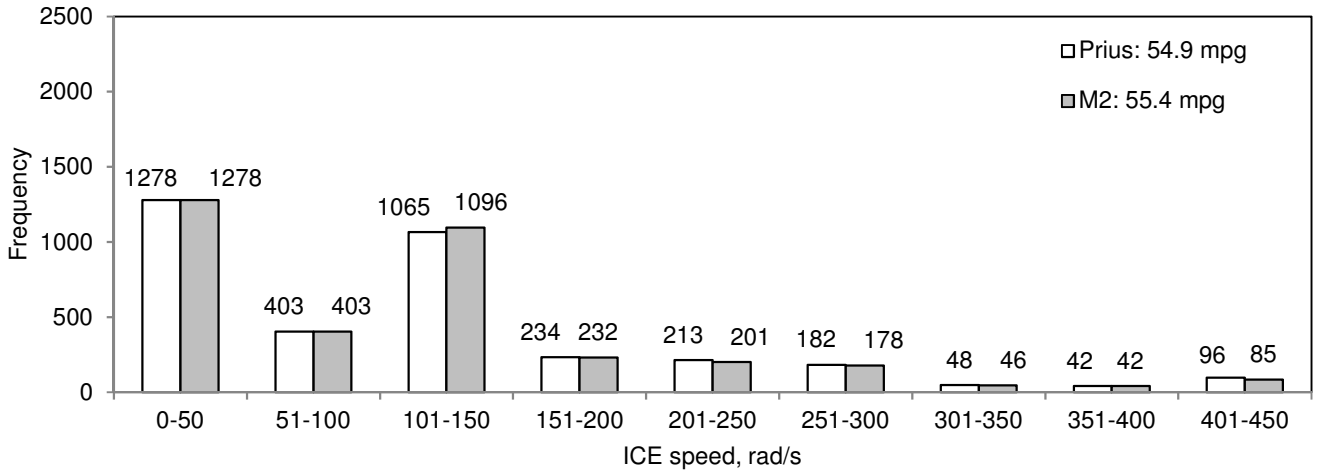

Figure 23: Distribution of ICE speed over D1: M2 design and Toyota Prius

Due to 4.5% lower power of the ICE and 28.3% lower capacity of the battery of the Toyota Prius compared to the M2 design, the Toyota Prius was required to operate more time at higher ICE torque and speed to achieve the desired final battery SOC. Therefore, more time of usage of the ICE in the Toyota Prius compared to the M2 design resulted in lower FE in the Toyota Prius compared to the M2 design.

As the FC over 60 Nm contributed to 86.3 and 87.3% of total FC for the M2 design and Toyota Prius respectively, 2.0% lower FC over 60 Nm due to 3.1% lesser time of operation over 60 Nm along with 5.0% lower time of operation of ICE over 200 rad/s caused 0.9% higher FE in the M2 design compared to the Toyota Prius over D1 driving pattern.

4. Conclusion

FE variability of the optimum designs generated by two design optimization methodologies were analysed statistically to understand the reasons for the variation. The analysis was carried out using a simulation model of a Toyota Prius non plug-in HEV for 10 real-world driving patterns over a predefined route consisting of urban and highway driving.

This study analyses the impacts of the parameters of driving patterns, such as, speed, acceleration, time of acceleration and deceleration and the operation of powertrains, such as, ICE, generator-motor, and battery on FE variability.

The driving time for acceleration and deceleration are one of the major reasons for FE variability in real-world driving. The higher driving time for acceleration and deceleration leads to lower FE and the lower driving time for acceleration and deceleration leads to higher FE.

The M2 design which optimized considering a range of different driving patterns, had lower FE variability compared to the benchmark vehicle, Toyota Prius without effecting average FE. The M2 design had higher FE compared to the benchmark vehicle, if driving patterns consisted of higher maximum speed and maximum acceleration. Hence, the M2 design had higher potential for better FE over aggressive driving patterns and more suitable for real-world applications compared to the Toyota Prius.

Due to bigger IC engine with the optimum combination of generator, motor and battery, the M2 design operates lesser time to charge the battery and therefore, has higher potential for better FE over more aggressive driving patterns. As the aggressive driving patterns are an important factors for higher FE variability, the M2 design has higher potential to have lower FE variability over different driving patterns.

The study shown that histogram plots of ICE operation over different driving patterns pinpoint the reason for higher FE variability and which operating regions need to be optimised. Although the study considered only FE as an optimization objective, the simillar statistical analysis is applicable while considering other parameters, such as, emission, cost, packaging etc. as additional objective functions.

No previous published research study has analysed statistically the reasons for the FE variability in real-world driving. This study provides a new dierction for systematic analyse of customers' concerns related to FE for real-world driving.

As the cost of components is another important factor to be considered for the optimum design of hybrid electric vehicle, the cost along with FE will be considered in further studies to understand its impact on the FE variability.

The experimental validation of the modelling will be considered in future study. Although the study considered driving patterns of 10 different drivers over a fixed route, the impact of more aggressive drivers will be studied in future.

5. References

1. Shafiee, S. and E. Topal, *When will fossil fuel reserves be diminished?* Energy Policy, 2009. **37**(1): p. 181-189.
2. Krewitt, W., et al., *Energy [R]evolution 2008--a sustainable world energy perspective.* Energy Policy, 2009. **37**(12): p. 5764-5775.
3. Ehsani, M., Y. Gao, and A. Emadi, *Modern electric, hybrid electric and fuel cell vehicles: fundamentals, theory and design.* CRC Press - Technology and Engineering, 2009.
4. Vallinayagam, R., et al., *Emission reduction from a diesel engine fueled by pine oil biofuel using SCR and catalytic converter.* Atmospheric Environment, 2013. **80**: p. 190-197.
5. Karner, D. and J. Francfort, *US department of energy hybrid electric vehicle battery and fuel economy testing.* Journal of Power Sources, 2006. **158**(2): p. 1173-1177.
6. Karner, D. and J. Francfort, *Hybrid and plug-in hybrid electric vehicle performance testing by the US Department of Energy Advanced Vehicle Testing Activity.* Journal of Power Sources, 2007. **174**(1): p. 69-75.
7. Alvarez, R. and M. Weilenmann, *Effect of low ambient temperature on fuel consumption and pollutant and CO2 emissions of hybrid electric vehicles in real-world conditions.* Fuel, 2012. **97**: p. 119-124.
8. Carlson, R., et al. *On-road evaluation of advanced hybrid electric vehicles over a wide range of ambient temperatures*. in *EVS23 International Battery, Hybrid and Fuel Cell Electric Vehicle Symposium*. 2007. California, .
9. Fontaras, G., P. Pistikopoulos, and Z. Samaras, *Experimental evaluation of hybrid vehicle fuel economy and pollutant emissions over real-world simulation driving cycles.* Atmospheric Environment, 2008. **42**(18): p. 4023-4035.
10. Carlson, R., et al., *Drive cycle fuel consumption variability of plug-in hybrid electric vehicles due to aggressive driving.* SAE Technical Paper 2009-01-1335, 2009.
11. Iwakuni, H., A. Takami, and K. Komatsu, *Development of Lean NOx Catalyst for Lean Bum Gasoline Engine.* Science and Technology in Catalysis, 1998: p. 251-256.
12. EPA, U.S., *Calculate or share your MPG.* U.S. Environment Protection Agency, 2012. [Online]. Available: http://www.fueleconomy.gov/mpg/MPG.do?action=browseList2&make=Toyota&model=Prius.
13. Ericsson, E., *Independent driving pattern factors and their influence on fuel-use and exhaust emission factors.* Transportation Research Part D, 2001. **6**(5): p. 325-345.
14. Yin, C., et al., *Fuzzy optimization of energy management for power split hybrid electric vehicle based on particle swarm optimization algorithm.* Advances in Mechanical Engineering, 2019. **11 (2)**: p. 1-12.
15. Li, Y., et al., *Parameters optimization of two-speed powertrain of electric vehicle based on genetic algorithm.* Advances in Mechanical Engineering, 2020. **12 (1)**: p. 1-16.
16. Metz, N., *Emission characteristics of different combustion engines in the city, on rural roads and on highways.* The Science of the Total Environment, 1993. **134**: p. 225-235.
17. Raykin, L., M.J. Roorda, and H.L. Maclean, *Impact of driving patterns on tank-to-wheel energy use of plug-in hybrid electric vehicle.* Transportation Research Part D, 2012. **17**: p. 243-250.
18. Sharer, P., R. Leydier, and A. Rousseau, *Impact of drive cycle aggressiveness and speed on HEVs fuel consumption sensitivity.* SAE Technical Paper 2007-01-0281, 2007.
19. Moawad, A., et al., *Impact of real world drive cycles on PHEV fuel efficiency and cost for different powertrain and battery characteristics.* International Battery, Hybrid and Fuel Cell Electric Vehicle

Symposium, EVS24, Stavenger, Norway, May 13 - 16, 2009: p. 1-10.
20. Galdi, V., et al., *A genetic-based methodology for hybrid electric vehicles sizing.* Soft Computing, 2001. **5**(6): p. 451-457.
21. Xudong, L., W. Yanping, and D. Jianmin. *Optimal sizing of a series hybrid electric vehicle using a hybrid genetic algorithm*. in *IEEE International Conference on Automation and Logistics*. 2007. Jinan, China, .
22. Yildiz, E.T., et al. *Nonlinear constraint component optimization of a plug-in hybrid electric vehicle*. in *The 25th World Battery, Hybrid and Fuel Cell Electric Vehicle Symposium & Exhibition, EVS25*. 2010. Shenzhen, China, .
23. Wu, X., et al., *Component sizing optimization of plug-in hybrid electric vehicles.* Applied Energy, 2011. **88**(3): p. 799-804.
24. Gao, W. and S.K. Porandla. *Design optimization of a parallel hybrid electric powertrain*. in *IEEE Vehicle Power and Propulsion Conference, VPPC '05*. 2005. Chicago, USA.
25. Desai, C. and S.S. Williamson. *Optimal design of a parallel Hybrid Electric Vehicle using multi-objective genetic algorithms*. in *IEEE Vehicle Power and Propulsion Conference, VPPC '09*. 2009. Dearborn, Michigan, USA.
26. Montazeri-Gh, M. and A. Poursamad, *Application of genetic algorithm for simultaneous optimisation of HEV component sizing and control strategy.* International Journal of Alternative Propulsion, 2006. **1**(1): p. 63-78.
27. Bingzhan, Z., et al. *Multi-objective parameter optimization of a series hybrid electric vehicle using evolutionary algorithms*. in *IEEE Vehicle Power and Propulsion Conference, VPPC '09*. 2009. Dearborn, Michigan, USA.
28. Lianghong, W., et al., *Multiobjective optimization of HEV fuel economy and emissions using the self-adaptive differential evolution algorithm.* IEEE Trans. Veh. Technol., 2011. **60**(6): p. 2458-2470.
29. Li-Cun, F. and Q. Shi-Yin. *Concurrent optimization for parameters of powertrain and control system of hybrid electric vehicle based on multi-objective genetic algorithms*. in *SICE-ICASE International Joint Conference*. 2006. Bexico, Busan, Mexico, .
30. Wu, J., C. Zhang, and N. Cui, *PSO algorithm-based parameter optimization for HEV powertrain and its control strategy.* International Journal of Automotive Technology, 2008. **9**(1): p. 53-59.
31. Gao, W. and C. Mi, *Hybrid vehicle design using global optimisation algorithms.* International Journal of Electric and Hybrid Vehicles, 2007. **1**(No. 1): p. 57-70.
32. Roy, H.K., A. McGordon, and P.A. Jennings, *A generalized powertrain design optimization methodology to reduce fuel economy variability in hybrid electric vehicles.* IEEE Trans. Veh. Tech., 2014. **63**: p. 1055-1070.
33. Roy, H.K., A. McGordon, and P.A. Jennings, *Reducing the variability of hybrid electric vehicle fuel economy in the real world.* Proc. IMechE, Part D: J. Automobile Engineering. , September 9, 2015.
34. Roy, H.K., A. McGordon, and P.A. Jennings, *Effect of Powertrain Design Optimisation Methodologies on Battery System Efficiency of a Hybrid Electric Vehicle*, in *SAE World Congress*2016: Detroit, USA.
35. Walker, A., et al. *A novel structure for comprehensive HEV powertrain modelling*. in *IEEE Vehicle Power and Propulsion Conference, VPPC '06*. 2006. Windsor, United Kingdom, .
36. Lieh, J., *A closed-form method to determine vehicle speed and its maximum value.* International Journal Vehicle Systems Modelling and Testing, 2008. **3**(1/2): p. 1-13.
37. Brayer, R., *Implementation of SAE standard J1666 May 93: Hybrid electric vehicle acceleration, gradeability and deceleration test procedure, ETA-HTP02*, 2004, Electric Transportation Applications, .
38. Holland, J.H., *Adaptation in natural and artificial system*1975: Ann Arbor, MI: University of Michigan Press.
39. Goldberg, D.E., *Genetic algorithms in search, optimization and machine learning*1989: Addison Wesley.
40. Cao, Y.J. and Q.H. Wu, *Teaching genetic algorithm using Matlab.* International Journal of Eletrical Engineering Education, 1999. **36**: p. 139-153.
41. Shojaei, A., et al. *Powertrain optimisation in a hybrid electric bus*. in *IEEE Vehicle Power and Propulsion Conference*. 2012. Seoul, Korea, .

Abbreviations

ECE15	Urban Driving Cycle
EUDC	Extra Urban Driving Cycle
FE	Fuel Economy
FTP-75	Federal Test Procedure 75
GA	Genetic Algorithm
HEV	Hybrid Electric Vehicle
HWFET	Highway Fuel Economy Test
ICE	Internal Combustion Engine

LA92	Los Angeles 92
NEDC	New European Driving Cycle
SOC	State Of Charge
US06	US Supplemental Test Procedure 06
WARPSTAR	Warwick Powertrain Simulation Tool for Architectures